Angular Momentum and Nuclear Shell Effects in Reactions of Ni^{58} with 46- to 68-MeV He^4 Ions*

MARSHALL BLANN AND GEORGE MERKEL
Department of Chemistry, The University of Rochester, Rochester, New York
(Received 4 March 1964; revised manuscript received 31 August 1964)

Excitation-function measurements are reported for reactions induced in Ni^{58} with 46–68-MeV helium ions. Targets were enriched to 99.95% Ni^{58}. The stacked-foil method followed by radiochemical separation was used to measure product yields resulting from the $(\alpha,\alpha n)$, $(\alpha,\alpha p)$, $(\alpha,\alpha 2n)$, $(\alpha,\alpha pn)$, $(\alpha,\alpha 2pn)$, $(\alpha,\alpha p2n)$, and $(\alpha,3pn)$ reactions. The experimental excitation functions (supplemented with previously reported cross sections for reactions of Ni^{58} with 14–48-MeV helium ions) were compared with three sets of statistical-theory calculations. The calculations differ in the dependence on energy and angular momentum assumed for the nuclear level density. In the first set of calculations the distribution of levels in the residual nuclei was assumed to be of the conventional form, $\rho(E,J)\propto(2J+1)(E-\delta)^{-2}\exp\{2[a(E-\delta)]^{1/2}\}$, where E is the excitation energy, J is the spin of the residual nucleus, δ is the pairing energy correction, and a is the level-density parameter. In the second set of calculations, the influence of nuclear shell structure on level densities was taken into consideration by the introduction of an energy shift ΔE as suggested by Rosenzweig. The residual nuclei are assumed to have a distribution of nuclear levels of the form $\rho(E,J)\propto(2J+1)(E-\delta+\Delta E)^{-2}\times\exp\{2[a(E-\delta+\Delta E)]^{1/2}\}$. In the third set of calculations [applied to the $(\alpha,\alpha p)$, $(\alpha,\alpha pn)$, and $(\alpha,\alpha p2n)$ excitation functions] the influence on level densities of large values of angular momentum was considered in a relatively simple manner. The residual nuclei were assumed to undergo classical rotation with energy of rotation, $E_{\rm rot}=I^2\hbar^2/2\mathcal{I}_{\rm rig}$, where I is the angular momentum introduced by the bombarding helium ion and $\mathcal{I}_{\rm rig}$ is the nuclear rigid-body moment of inertia. The rotational energy was assumed to be dissipated by γ-ray emission (with $J=I$ throughout the evaporation process). Essentially, the residual nuclei were assumed to have a distribution of levels given by an expression of the form $\rho(E,J)\propto(2J+1)(E-\delta E-_{\rm rot})\times\exp\{2[a(E-\delta-E_{\rm rot})]^{1/2}\}$. The pairing energy δ was calculated from experimental mass values; the level-density parameter used was $a=7.0$ MeV^{-1}, the value measured by Sherr and Brady from $Ni^{58}(p,\alpha)$ spectra. Nonelastic cross sections calculated with the nuclear optical model were used for inverse cross sections. The relationship of the third set of calculations to the compound-nucleus theory of Ericson and Strutinski is discussed. An estimate of the error resulting from the use of the simple rotational energy model rather than the more rigorous theory of Ericson and Strutinski is presented.

I. INTRODUCTION

A NUMBER of investigations of medium energy compound-nucleus reactions in the region $A\sim60$ have been reported. These measurements include total reaction cross sections,[1] energy and angular distributions of emitted particles,[2–7] excitation functions,[8–12] and recoil-range measurements.[13,14] In this work we report the measurement of $(\alpha,\alpha n)$, $(\alpha,\alpha 2n)$, $(\alpha,\alpha p)$, $(\alpha,\alpha pn)$, $(\alpha,\alpha 2pn)$, $(\alpha,\alpha 2np)$, and $(\alpha,3pn)$ excitation functions of Ni^{58} induced with 46- to 68-MeV helium ions. The experimental results are interpreted in terms of the statistical theory.[15–17]

Angular distributions for (α,α') reactions in the region $A\sim60$ are consistent with total reaction cross sections that are produced predominantly by the compound nucleus reaction mechanism.[4,5] Mean recoil-range measurements of most of the final residual nuclei produced by the above reactions have been reported.[14] The mean recoil ranges may be used to determine whether or not specific reactions are consistent with a compound nucleus mechanism; i.e., the recoil-range measurements provide a criterion for determining which specific excitation functions, or what part of a specific excitation function, cannot properly be analyzed by the statistical theory.

Two principal considerations motivated this extension of previous measurements[12] to higher excitation energies. First, we wanted to obtain additional data on compound nucleus reactions in the region of the doubly closed shell Ni^{56} nucleus. Our interest in reactions in the Ni^{58} region arises from the small measured cross sections for the $Ni^{58}(\alpha,\alpha 2n)Ni^{56}$ and $Ni^{58}(\alpha,\alpha n)Ni^{57}$ excitation functions; these yields are small both with respect to the corresponding $Ni^{58}(\alpha,\alpha pn)Co^{56}$ and $Ni^{58}(\alpha,\alpha p)Co^{57}$ reactions,

* This work was supported by the U. S. Atomic Energy Commission.

[1] G. Igo and B. Wilkins, Phys. Rev. **131**, 1251 (1963).
[2] H. W. Fulbright, N. O. Lassen, and N. O. Roy Poulsen, Kgl. Danske Videnskab. Selskab, Mat.-Fys. Medd. **31**, No. 10 (1959).
[3] R. Sherr and F. P. Brady, Phys. Rev. **124**, 1928 (1961).
[4] G. Merkel, University of California Lawrence Radiation Laboratory Report UCRL-9898, 1962 (unpublished).
[5] J. Benveniste, G. Merkel, and A. Mitchell, Bull. Am. Phys. Soc. **7**, 454 (1962).
[6] Richard W. West, thesis, Department of Physics, University of Washington, 1963 (unpublished).
[7] D. Bodansky, R. K. Cole, W. G. Cross, C. R. Gruhn, and I. Halpern, Phys. Rev. **126**, 1082 (1962).
[8] F. S. Houck and J. M. Miller, Phys. Rev. **123**, 231 (1961).
[9] S. Tanaka, J. Phys. Soc. Japan **15**, 2159 (1960).
[10] E. A. Bryant, D. R. F. Cochran, and J. D. Knight, Phys. Rev. **130**, 1512 (1963).
[11] M. Blann and G. Merkel, Phys. Rev. **131**, 764 (1963).
[12] M. Blann and G. Merkel, Nucl. Phys. **52**, 673 (1964).
[13] J. B. J. Read, I. Ladenbauer-Bellis, and R. Wolfgang, Phys. Rev. **127**, 1722 (1962).
[14] M. Blann and A. Ewart, Phys. Rev. **134**, B783 (1964).
[15] V. F. Weisskopf, Phys. Rev. **52**, 295 (1937).
[16] L. Wolfenstein, Phys. Rev. **82**, 690 (1951).
[17] A. M. Lane and R. G. Thomas, Rev. Mod. Phys. **30**, 257 (1958).

and with respect to the predictions of a statistical theory calculation which neglects the effect of nuclear shell structure on level densities. The second reason for undertaking this work was to study the influence of the high angular momenta of the compound nuclei on the resulting excitation functions.

Statistical theory calculations have been reported for the $(\alpha,\alpha n)$, $(\alpha,\alpha p)$, $(\alpha,\alpha pn)$, and $(\alpha,\alpha 2n)$ excitation functions of Ni^{58} with 14–48-MeV helium ions.[12] In this work we extend these calculations to 68-MeV incident helium ion energy. These calculations are based on the assumption that residual nuclei have spin distributions proportional to $(2J+1)$; we have not considered the influence of nuclear shell structure on level densities in this first set of calculations. In a second set of calculations we employ the level-density expression derived by Rosenzweig to estimate the influence of shell structure on level densities.[18,19] Rosenzweig used a simplified model of the nucleus to obtain a closed form nuclear level-density expression which takes nuclear shell structure into consideration. His result differs from the standard Fermi gas level-density expression[20–22] by a constant shift in excitation energy. The second set of calculations is also based on the assumption that the residual nuclei have spin distributions proportional to $(2J+1)$.

In a third set of calculations we attempt to consider the influence of the large values of angular momentum on the decay of the compound nuclei. Ideally we would like to base our calculation on a spin distribution of the form $\rho(J) \propto (2J+1)\exp(-J^2/2\sigma^2)$, where σ^2 is the spin-cutoff parameter.[23] When multiple particle emission can take place (and in the reactions of this work as many as five particles are emitted) a rigorous calculation of compound nucleus decay with an exponential spin-cutoff-dependent level density becomes a practical impossibility because of the computer time requirement. We therefore use a simplified model to gain insight into the more complex calculation. The compound nucleus is assumed to undergo classical rotation for each impact parameter; it is assumed that all rotational energy is eventually dissipated as γ radiation. This model is used to calculate the $(\alpha,\alpha p)$, $(\alpha,\alpha pn)$, and $(\alpha,\alpha p2n)$ excitation functions, since these are representative of the $(\alpha,\alpha x$ nucleon) reactions of this work. Finally we discuss the relationship between the simplified calculation of this work and the treatment of Ericson and Strutinski, and estimate the errors introduced by the calculation of this work.

[18] N. Rosenzweig, Phys. Rev. **108**, 817 (1957).
[19] N. Rosenzweig, Phys. Rev. **105**, 950 (1957).
[20] H. A. Bethe, Rev. Mod. Phys. **9**, 69 (1937).
[21] T. Ericson, in *Proceedings of the International Conference on Nuclear Structure, Kingston, Canada, 1960*, edited by D. A. Bromley and E. Vogt (University of Toronto Press, Toronto, 1960), p. 697.
[22] D. W. Lang, Nucl. Phys. **26**, 434 (1961).
[23] T. Ericson and V. Strutinski, Nucl. Phys. **8**, 284 (1958).

II. EXPERIMENTAL PROCEDURES

A. Targets

Targets were prepared by electroplating 99.95% enriched Ni^{58} onto 0.2-mil gold foils. Each gold cathode was individually weighed and measured prior to use to determine thickness; thicknesses varied between 9.3 and 10.0 mg/cm^2. The plating chimneys used gave 1.90-cm-diameter circular plates. The Ni^{58} target thicknesses varied between 4.07 and 9.52 mg/cm^2. The catcher-degrader foils used were 99.5% pure aluminum, 2.02 mg/cm^2 thick. The two target stacks used consisted of alternate aluminum foils and nickel-plated gold foils; there were, additionally, iron-plated gold foils in the stack. Reactions in the iron-plated foils will not be discussed in this work. Each target stack contained ten nickel-plated targets (and nine 2–4-mg/cm^2 iron-plated targets). Targets were arranged with the nickel facing away from the gold foils and beam direction and toward the aluminum catcher foils. Each of the two complete target stacks was wrapped in a single layer of 5.0-mg/cm^2 aluminum foil for ease of handling.

B. Bombardments

Bombardments were performed on the University of California Lawrence Radiation Laboratory 88-in. spiral ridge cyclotron. Two consecutive helium ion bombardments were run, each of approximately 15 min duration. Targets were bombarded in a 0° port 33 ft from the accelerator. A $\frac{1}{2}$-in.-diam graphite collimator was placed 1 ft in front of the target holder. The target holders served as Faraday cups for the two runs. Unfortunately there was a malfunction in the beam-current integrating system during the first bombardment. The integrated beam current on the second run was 0.300 μA·h. To calculate the beam current on the first target stack, Na^{22} activity was measured in the aluminum envelopes of the two targets. The ratio of activities in the 1.26-MeV photopeak of Na^{22} was $(0.272\pm0.004):1.00$, indicating that the first target received 0.111 ± 0.001 μA·h integrated beam current. The deviations we quote for the beam-current measurements are precision estimates; accuracy should be $\pm 10\%$ or better. The absolute cross sections of this work are dependent on a single beam-current measurement; however, between 46 and 48 MeV bombarding energy the excitation functions for formation of Ni^{56}, Ni^{57}, Co^{56}, and Co^{57} overlap previously measured excitation functions. The latter values were based on six beam-current measurements, and are in turn in agreement with measured values due to Houck and Miller[8] and Tanaka.[9] We therefore have no reason to doubt the accuracy of the beam-current values used for the bombardments of this work.

The energy of the incident helium-ion beam was calculated to be 69 ± 1 MeV.[24] The calculation was based on

[24] H. Grunder (private communication).

the extraction radius and cyclotron frequency. The calculated values were found to be in good agreement with energy determinations based on aluminum range measurements.[24]

C. Chemistry

Targets and their respective catcher foils were dissolved separately in 8*M* HCl solutions to which carriers of Ni, Co, Fe, and Mn had been added. Ten milligrams of Na carrier was added to each sample as a holdback carrier. The resulting solutions were run through Dowex-1 anion exchange columns, which were rinsed with equal volumes of 8*M* HCl. Cobalt and iron complexes were retained on the resin; all other ions were in the eluant. Cobalt was removed from the column with 4*M* HCl, and was precipitated as $K_3Co(NO_2)_6 \cdot H_2O$. Iron was removed with 0.1*M* HCl and was precipitated and mounted as the salt of 8-hydroxyquinoline.

Five milligrams of Co carrier was added to each nickel sample eluted from the columns. After five days the solutions were again separated by ion exchange as in the initial separation described above. In this time 90% of the Ni^{57} had decayed to Co^{57}, making spectroscopy for Ni^{56} experimentally simpler. The eluted solution containing Ni, Mn, Al, and Na was made basic with an excess of NaOH, precipitating hydroxides of Ni and Mn. The hydroxides were dissolved in a minimum volume of 6*N* HCl. The resulting solution was made alkaline with an excess of NH_4OH. Several drops of 3% H_2O_2 were added to the ammoniacal solution to oxidize manganese to the +4 oxidation state, in which form manganese hydroxide is insoluble in ammonia. The resulting $Ni(NH_3)_4^{++}$ solution was diluted with distilled water and excess dimethylglyoxime was added to precipitate nickel. Separation of Ni and Mn was necessary because of the similarity of half-lives and γ-ray spectra of Ni^{56} and Mn^{52}; tracer amounts of Mn would coprecipitate with nickel dimethylglyoxime if no prior separation had been performed.

D. Cross-Section Determinations

Characteristics of radiation detected in the cross-section measurements of this work are summarized in Table I. Positrons were counted with an end-window proportional counter which had been calibrated by the method of Bayhurst and Prestwood.[25] Gamma scintillation spectrometry was performed with a 512-channel pulse-height analyzer with 3×3-in., $1\frac{1}{2}$×1-in., and $1\times\frac{1}{32}$-in. crystals. The latter crystal had a 5-mil Be window and was used solely to count Fe^{55} *K* x rays. Crystal efficiency curves determined by Heath and by Hollander and Kalkstein were used to calculate absolute crystal efficiencies.[26,27] Helium ion energy as a function of target stack depth was calculated from the theoretical proton-range values of Barkas[28] with the relation[29]

$$R_{M,Z}(E) = (M/Z^2)R_p(E/M),$$

where $R_{M,Z}(E)$ represents the range of an ion of mass M, charge Z, and energy E, and $R_p(E/M)$ represents the range of a proton of energy E/M.

Sodium-24 contamination (from Al catcher foils) is a possible source of error in determining Co^{55} cross sections from β^+ activity. To check this γ spectra were taken of all Co samples from catcher foils. No trace of Na^{24} contamination was found.

Activities in catcher foils and target foils were summed to obtain final results. Corrections were applied, where applicable, for genetic relationships, gamma-gamma coincidences, and (for Fe^{55} *K* x rays) self-absorption and window absorption. We estimate the cross sections reported in this work to be accurate to ±25%, with the exception of cross sections for Fe^{55}. The accuracy of the latter excitation function is estimated to be ±40%. The experimentally determined cross sections are listed in Table II.

TABLE I. Decay characteristics of isotopes studied in this work.[a]

Nuclide	Type of radiation observed	Energy of radiation observed (MeV)	Assumed abundance (per decay)	Assumed half-life
Ni^{56}	γ	0.164	0.99	6.1 d[b]
Ni^{57}	β^+		0.50	36.0 h
Co^{55}	β^+		0.60	18.2 h
Co^{56}	γ	1.26	0.70	77 d
Co^{57}	γ	0.120	1.00	270 d
Co^{58}	γ	0.810	1.00	71 d[c]
Fe^{52}	β^+		1.56	8.3 h
Fe^{55}	*K* x ray	0.0059	0.28	2.6 y[d]

[a] D. Strominger, J. M. Hollander, and G. T. Seaborg, Rev. Mod. Phys. **30**, 585 (1958), unless otherwise referenced.
[b] D. O. Wells, S. L. Blatt, and W. E. Meyerhof, Phys. Rev. **130**, 1961 (1963).
[c] The 0.810-MeV photopeak area represented the yield of Co^{56} and Co^{58}. The fraction of the peak due to Co^{56} was calculated from the area of the 1.26-MeV peak and subtracted from the total 0.810-MeV peak area to obtain the Co^{58} contribution.
[d] C. D. Broyles, D. A. Thomas, and S. K. Haynes, Phys. Rev. **89**, 715 (1953).

III. STATISTICAL THEORY CALCULATIONS

A. Conventional Statistical Theory

The first set of calculations was made with the assumption that the spin dependence of nuclear level densities in the residual nuclei is described by

$$\rho(E,J) \propto (2J+1)\rho(E), \qquad (1)$$

where E is the excitation energy and J is the spin of the residual nucleus. With the assumption of Eq. (1),

[25] B. P. Bayhurst and R. J. Prestwood, Nucleonics **17**, 82 (1959).
[26] R. L. Heath, Atomic Energy Commission Research and Development Report IDO 16408, 1957 (unpublished).
[27] J. M. Hollander and M. Kalkstein, University of California Radiation Laboratory Report UCRL-2764, 1954 (unpublished).
[28] W. H. Barkas, University of California Lawrence Radiation Laboratory Report UCRL-10292, 1962 (unpublished).
[29] B. G. Harvey, *Introduction to Nuclear Physics and Chemistry* (Prentice-Hall Inc., Englewood Cliffs, New Jersey, 1962), Chap. 11, p. 223.

TABLE II. Experimental cross sections measured in this work.

Helium ion energy (MeV)[a]	Reaction:	Cross section (mb) for the production of: Ni^{56} $(\alpha,\alpha 2n)$	Ni^{57} $(\alpha,\alpha n)$	Co^{55} $(\alpha,\alpha p2n)$	Co^{56} $(\alpha,\alpha pn)$	Co^{57} $(\alpha,\alpha p)$	Co^{58} $(\alpha,3pn)$	Fe^{55} $(\alpha,\alpha p2n)$
67.8[b]		2.3	31	53	71	151	213	
67.1		2.6	35	49	70	133	198	119
65.7[b]		2.7	39	42	65	100	185	
64.9		2.6	34	43	71	104	156	103
63.3[b]		2.3	28	32	59	73	146	
62.8		2.4	32	37	80	87	190	96
61.0[b]		2.2	25	29	79	65	170	
60.6		2.2	26	31	91	71	193	86
59.1[b]		2.4	25	27	91	64	195	
58.4		2.5	26	24	106	63	191	75
56.9[b]		2.6	26	22	124	59	194	
56.1		2.6	26	17	122	62	170	57
54.7[b]		2.6	25	15	138	60	168	
53.8		2.3	23	10	130	57	91	37
52.3[b]		2.7	28	11	170	69	148	
51.2		2.6	28	7.1	158	66	115	20
49.8[b]		2.0	23	3.4	143	64	90	
48.7		1.8	26	2.8	150	73	70	1.1
47.4[b]		1.5	23	1.4	137	69	39	
46.1		1.4	27	0.9	136	79	34	

[a] The energy listed is the calculated average helium ion energy in each target foil. The maximum target thickness was 0.8 MeV; the mean target thickness was 0.6 MeV. These values were calculated with the range curves derived from Ref. 28 and neglect straggling.
[b] First bombardment.

the probability per unit time of emitting a particle ν with kinetic energy between ϵ and $\epsilon+d\epsilon$ (from a nucleus at excitation E^*) is given by

$$P_\nu(E^*,\epsilon)d\epsilon=\gamma_\nu\sigma_{\rm inv}(\epsilon_\nu)\frac{\rho(E)}{\rho(E^*)}d\epsilon, \qquad (2)$$

where $\gamma_\nu=(g_\nu m_\nu/\pi^2\hbar^3)$, g_ν is the number of spin states of particle ν, m_ν is the reduced mass of particle ν, $\rho(E)/\rho(E^*)$ is the ratio of level densities at excitation energies E and E^*, and $\sigma_{\rm inv}(\epsilon_\nu)$ is the cross section for the capture of particle ν with channel energy between ϵ and $\epsilon+d\epsilon$ by the residual nucleus at excitation E to form the initial nucleus with excitation energy E^*.[15,30]

We have assumed a nuclear level density expression of the form[21,22]

$$\rho(E)\propto(E-\delta)^{-2}\exp\{2[a(E-\delta)]^{1/2}\} \qquad (3)$$

where the influence of odd-even properties of nuclei has been corrected for with an excitation energy shift δ.[31–33]

Before Eqs. (2) and (3) can be used in actual calculations, values of the parameters a, $\sigma_{\rm inv}(\epsilon_\nu)$, and δ must be selected. The values of these parameters were selected from independent experimental work, where such information was available. These values were used with several computer programs[11,12,34] to calculate cross sections for n, p, and α emission. Competition from d, t, and He^3 evaporation was taken into consideration for the first two particles emitted in the cascade.

1. Level-Density Parameter

The level-density parameter used in these calculations, $a=7.0$ MeV^{-1}, was determined from α-particle spectra resulting from the $Ni^{58}(p,\alpha)Fe^{55}$ reaction.[3] The α-particle spectra were analyzed with a level density expression of the form given by Eq. (3).

2. Pairing Energy Correction

The parameter δ was taken to be a pairing energy and was evaluated from graphs of $M-A$ versus Z for several isobars in the $A=60$ region. The experimentally determined masses reported by Everling *et al.* were used.[35] For odd-odd nuclides we assumed $\delta=0$ MeV; for odd-even nuclides, $\delta=1.4$ MeV; and for even-even nuclides, $\delta=2.8$ MeV.

3. Inverse Reaction Cross Sections

Values of $\sigma_{\rm inv}(\epsilon_\nu)$ have been calculated with the nuclear optical model. When the optical-model theory is used to calculate $\sigma_{\rm inv}(\epsilon_\nu)$, the optical-model nonelastic-reaction cross section is assumed to be equal to the compound-nucleus inverse cross section. Actually, optical-model nonelastic-reaction cross sections consist of the sum of all inelastic cross sections plus compound elastic cross sections, and not all inelastic reactions result in the formation of a compound nucleus. Another difficulty

[30] G. R. Satchler, in Proceedings of the Conference on Reactions Between Complex Nuclei, Gatlinburg [Oak Ridge National Laboratory Report ORNL-2606, 1958 (unpublished)], p. 79.
[31] H. Hurwitz and H. Bethe, Phys. Rev. **81**, 898 (1951).
[32] T. D. Newton, Can. J. Phys. **34**, 804 (1956).
[33] T. Ericson, Nucl. Phys. **6**, 62 (1958).
[34] M. Blann, Phys. Rev. **133**, B707 (1964).
[35] F. Everling, L. A. Konig, J. H. E. Mattauch, and A. H. Wapstra, Nucl. Phys. **18**, 529 (1960).

arises because the experimentally determined optical-model parameters available apply only to target nuclei in their ground state. The inverse cross section most frequently corresponds to the formation of a compound nucleus by the collision of a bombarding particle with a highly excited target nucleus. Unfortunately, the variation of the optical-model parameters as a function of target excitation is not known.

Ericson has suggested that nuclear transparency decreases with increasing excitation energy; his argument is based on the Pauli exclusion principle.[36] For this reason we have used an imaginary potential deeper than that determined from elastic neutron scattering in our calculation of neutron inverse cross sections. The parameter values actually used give results for neutron-capture cross sections which are in good agreement with the continuum theory values.[37] For protons and α particles we have used published values of optical-model parameters.[38,39] The parameters used have been summarized previously.[11–12]

Transmission coefficients for formation of the compound nuclei were calculated with the optical-model parameters of Darriulat *et al.*[40]

B. Influence of Nuclear Shell Structure on Level Densities

The residual nuclei of interest in this work are in the region of the doubly closed shell Ni^{56} nucleus. There is both experimental evidence and theoretical justification for believing that nuclear shell structure can have an important effect on nuclear level densities.[18,19] The existence of nuclear shell effects at high excitation energies was first predicted by Margenau.[41] Subsequent theoretical treatments have been presented by Bloch[42] and Rosenzweig.[18,19]

Bloch applied the methods of statistical mechanics to the nuclear shell model in order to calculate the effect of nuclear shell structure on nuclear level densities at relatively high excitation energies. His results are, however, relatively unwieldy. Rosenzweig, by employing a simplified nuclear model, obtained a closed-form expression which illustrates the shell effects considered by Margenau and Bloch. In Rosenzweig's model the nucleus consists of two kinds of Fermi particles, each occupying uniformly spaced energy levels. The degeneracy of each level is the same, although the degeneracies for the different particles, i.e., neutrons and protons, can be different. For the neutron system, let n be the number of neutrons in the top Fermi level, g the degeneracy of each neutron level, and γ the spacing between adjacent levels. For the proton system, let p be the number of protons in the Fermi level, e the degeneracy of each level, and ϵ the spacing between adjacent levels. If we set $\Delta_n=\gamma/g$, $\Delta_p=\epsilon/e$, and $\Delta^{-1}=\Delta_n^{-1}+\Delta_p^{-1}$, Rosenzweig's total level density expression is given by

$$\rho(E)=\frac{1}{4}\left(\frac{\Delta_n^2\Delta_p^2}{216(E+\Delta E)^5\Delta^3}\right)^{1/4}\times\exp\left[\pi\left(\frac{2(E+\Delta E)}{3\Delta}\right)^{1/2}\right], \quad (4)$$

where

$$\Delta E=\frac{g\gamma}{12}-\frac{\gamma}{2g}(n-\tfrac{1}{2}g)^2+\frac{e\epsilon}{12}-\frac{\epsilon}{2e}(p-\tfrac{1}{2}e)^2 \quad (5)$$

and E is the excitation energy of the nucleus.

In order to calculate the value of the energy shift ΔE in the nuclear mass region of Ni^{56} we have averaged the number of states in the $2p_{3/2}$ and $1f_{7/2}$ subshells and set the degeneracy parameters of Eq. (5) equal to this average, i.e., $g=e=6$ (if the closely lying $2p_{3/2}$ and $1f_{5/2}$ subshells were combined before averaging with the $1f_{7/2}$ subshell the average would be 7.5). For the value of the nuclear spacings, γ and ϵ, we have used the energy difference between the $2p_{3/2}$ and $1f_{7/2}$ subshells as given in the Nilsson nuclear level scheme for a spherical nucleus.[43] If we assume[43] that $\hbar\omega_0=(41)A^{-1/3}$, the nucleon level scheme of Nilsson gives a difference of 3 MeV between these subshells. With the above parameters Eq. (5) simplifies to

$$\Delta E=3-\tfrac{1}{4}(n-3)^2-\tfrac{1}{4}(p-3)^2 \quad (6)$$

The second set of calculations was performed with Eq. (3) modified to

$$\rho(E,J)\propto(2J+1)(E+\Delta E-\delta)^{-2}\times\exp 2(E+\Delta E-\delta)^{1/2}. \quad (7)$$

In the second set of calculations we have assumed that there will be no particle emissions that populate residual nuclei in the region $E+\Delta E-\delta\leq 0$.

We have not derived Eq. (7) from first principles. Whether the energy-dependent term preceding the exponential term is to the -2 power as in Eq. (7) or to the $-5/4$ power as in Eq. (4) does not significantly affect the value of the calculated excitation function. The combination of the Rosenzweig energy shift and the pairing energy shift in Eq. (7) can only be justified on phenomenological grounds. Bloch has shown, however, that the effect of symmetry-dependent nuclear forces can be considered with a simple energy shift.[42]

[36] T. Ericson, in *Advances in Physics*, edited by N. F. Mott (Taylor and Francis, Ltd., London, 1960), Vol. 9, p. 425.
[37] J. M. Blatt and V. F. Weisskopf, *Theoretical Nuclear Physics* (John Wiley & Sons, Inc., New York, 1952).
[38] F. E. Bjorklund and S. Fernbach, in *Proceedings of the Second United Nations International Conference on the Peaceful Uses of Atomic Energy, Geneva, 1958* (United Nations, Geneva, 1958), Vol. 14, p. 24.
[39] J. R. Huizenga and G. J. Igo, Nucl. Phys. **29**, 462 (1962).
[40] R. Darriulat, G. Igo, H. G. Pugh, J. M. Meriwether, and S. Yamabe, Phys. Rev. **134**, B42 (1964).
[41] H. Margenau, Phys. Rev. **59**, 627 (1941).
[42] C. Bloch, Phys. Rev. **93**, 1094 (1954).
[43] S. C. Nilsson, Kgl. Danske Videnskab. Selskab, Mat. Fys. Medd. **29**, No. 16 (1955).

C. Influence of High Angular Momentum Values on Excitation Function Calculations

In this section we estimate the influence of the relatively large values of angular momentum encountered with 46–68-MeV incident helium ions. We describe a relatively crude but tractable procedure that is used to estimate the effect of large angular momentum values on the decay of a compound nucleus. We then discuss the relation of the simplified procedure to the more rigorous theory of Ericson and Strutinski.[23] Finally we attempt to estimate the divergence between the results of our simplified procedure and a more rigorous calculation.

1. Approximation of Angular Momentum Effects

Let an excitation function calculated as in Sec. II.B with Eq. (2) be given by

$$\sigma_{\text{c.n.}}(E_\alpha)=\pi\lambda\!\!\!^{-2}\sum(2I+1)T_I(E_\alpha)P_f(E^*) \qquad (8)$$

where $T_I(E_\alpha)$ is the transmission coefficient of the bombarding helium ion with energy E_α and angular momentum I, and where $P_f(E^*)$ is the probability of the formation of the residual nucleus f by multiple particle emission from a compound nucleus at excitation energy E^*.

We attempt to estimate the influence of large angular momentum values on the decay of the compound nucleus by making two simplifying assumptions: First we assume that the population of successive residual nuclei produced by particle emission remains proportional to $(2I+1)T_I(E_\alpha)$; second, we assume that the various residual nuclei behave as rigid rotors[44] with moment of inertia $\mathcal{I}_{\text{rig}}$. Then if a helium ion with angular momentum I impinges on the target, the final residual nucleus produced by particle emission has a rotational energy equal to $\hbar^2I^2/2\mathcal{I}_{\text{rig}}$. We assume

$$\sigma_{\text{c.n.}}(E_\alpha)=\pi\lambda\!\!\!^{-2}\sum(2I+1)T_I(E_\alpha)P_f(E^*-\hbar^2I^2/2\mathcal{I}_{\text{rig}}). \qquad (9)$$

2. Theory of Ericson and Strutinski

Ericson and Strutinski in their semiclassical derivation of compound nucleus cross sections use a residual nucleus spin and energy dependence of the form[23]

$$\rho(E,J)=\rho(E,0)(2J+1)\exp(-J^2/2\sigma^2), \qquad (10)$$

where E is the excitation energy and J the angular momentum of the residual nucleus.

If the compound nucleus with excitation energy E^* and angular momentum I has a nuclear level distribution given by $\rho_c(E^*,I)$, then the probability per unit time of emitting a particle ν with kinetic energy ϵ is given by[23]

$$P_\nu(E^*,I,\epsilon)=\frac{g_\nu\rho(E,0)}{\rho_c(E^*,I)\hbar}\int_0^\infty 2lT_l{}^\nu(\epsilon)\exp[-(I^2+l^2)/2\sigma^2]\times j_0(ilI/\sigma^2)dl, \qquad (11)$$

where $T_l{}^\nu(\epsilon)$ is the transmission coefficient of a particle ν with kinetic energy ϵ and angular momentum l, g_ν is the number of spin states of the particle, and j_0 is the spherical Bessel function of order 0. In the case of the rigid-rotor nuclear model the spin cutoff parameter σ^2 is given by

$$\sigma^2=\mathcal{I}_{\text{rig}}T/\hbar^2$$

where $\mathcal{I}_{\text{rig}}$ is the rigid body moment of inertia and $T=(E/A)^{1/2}$ is the thermodynamic temperature of the nucleus.

3. Relationship of Eq. (9) to the Theory of Ericson and Strutinski

As indicated in the introduction, an application of Eq. (11) to the calculation of excitation functions involving multiple emission of particles would be extremely unwieldy. We therefore use the simplified method described by Eq. (9). Equation (9) can be obtained from Eq. (11) by making two simplifying approximations: The first approximation is

$$\exp(-l^2/2\sigma^2)j_0(iIl/\sigma^2)\approx 1. \qquad (12)$$

The second is that the population of the spin states of all the residual nuclei produced in the particle emission cascade is the same as the distribution of states in the original compound nucleus. These assumptions are rigorously correct only for the case of s wave emission from the compound nucleus. [In the following subsection we present an attempt to estimate the error introduced by the use of the simplified calculation procedure based on Eq. (9).]

With the assumption of Eq. (12), Eq. (11) becomes

$$P_\nu(E^*,I,\epsilon)=\frac{g_\nu\rho(E,0)\exp(-I^2/2\sigma^2)}{\rho_c(E^*,I)\hbar}\epsilon_\nu\sigma_{\text{inv}}(\epsilon_\nu), \qquad (13)$$

where

$$\sigma_{\text{inv}}(\epsilon_\nu)\cong\pi\lambda\!\!\!^{-2}\sum_{l=0}^{\infty}(2l+1)T_l(\epsilon_\nu).$$

From the rigid-rotor-model value of σ^2 we obtain

$$\rho(E,0)e^{-I^2/2\sigma^2}=\rho(E,0)\exp(-\hbar^2I^2/2\mathcal{I}_{\text{rig}}T). \qquad (14)$$

Equation (14) plus an expansion of Eq. (7) in terms of nuclear temperature yields

$$\rho(E,0)e^{-I^2/2\sigma^2}\cong\rho(E-\hbar^2I^2/2\mathcal{I}_{\text{rig}},0), \qquad (15)$$

where, when $E\gg-\delta-\hbar^2I^2/2\mathcal{I}_{\text{rig}}$, $T\approx E/[(aE)^{1/2}-2]\approx(E/a)^{1/2}$. Expressions (13) and (15) can then be

[44] A radius parameter of 1.2 F was used in calculating the rigid-body moment of inertia. Experimental justification for the values reported was discussed by J. Benveniste, G. Merkel, and A. Mitchell, Bull. Am. Phys. Soc. **9**, 93 (1964).

combined to yield

$$\rho_\nu(E^*,I,\epsilon)\cong\frac{g_\nu\rho_\nu(E-\hbar^2I^2/2\mathcal{I}_{\rm rig},0)\epsilon_\nu\sigma_{\rm inv}(\epsilon_\nu)}{\rho_c(E^*,I)\hbar}. \quad (16)$$

Equation (9) follows from Eq. (16) with the assumption that the population of spin states in residual nuclei remains proportional to $(2I+1)T_I(E_\alpha)$.

When the multiple-particle decay-mode probabilities $P_f(E^*-\hbar^2I^2/2\mathcal{I}_{\rm rig})$ of Eq. (9) that correspond to large values of I make important contributions to expression (9), the magnitude of $\sigma_{\rm c.n.}(E_\alpha)$ is sensitive to the assumptions used to obtain $T_I(E_\alpha)$. Optical-model reaction-transmission coefficients which are based on experimental parameters would overestimate the probability for the compound-nucleus formation because the optical-model values correspond to all inelastic processes, not just compound-nucleus reactions. For this reason the results of these calculations, where we have used optical-model transmission coefficients, are expected to be extreme estimates of the influence of angular momentum on level densities (extreme within the limitations of the assumptions we have made).

4. *Validity of Calculations Based on Eq. (9)*

In this subsection we attempt to obtain an estimate of the divergence between a calculation based on Eq. (11) and a calculation based on Eq. (9). We start by examining the validity of Eq. (12) for several critical values of I, l, and σ^2. The expression that appears on the left side of Eq. (12),

$$\exp(-l^2/2\sigma^2)j_0(iIl/\sigma^2), \quad (17)$$

increases with increasing values of I and l, and decreasing values of σ^2. In our examination of the validity of the approximation of Eq. (12) we choose values of I and σ^2 which yield an upper limit to the errors introduced by this approximation. Figure 1 shows the value of expression (17) for $I=I_{\rm max}$ (see below) and for σ^2 corresponding to a residual nucleus excitation energy equal to one-half the initial compound nucleus excitation energy. This value of σ^2 was chosen to correspond to the case of emission of one or two nucleons before the emission of an alpha particle. Since optical-model values of I extend to very high values as T_I approaches 0, we have calculated $I_{\rm max}$ from a classical sharp-cutoff model with $R_0=1.5$ F, i.e.,

$$I_{\rm max}=0.245E_\alpha(1-14.8/E_\alpha)^{1/2}.$$

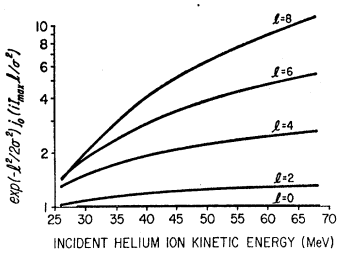

FIG. 1. Variation of the value of expression (17) as a function of bombarding energy for a number of emitted particle angular momentum quantum numbers. The spin cutoff parameter was calculated with the assumption that the excitation energy of the residual nucleus was equal to one-half the excitation energy of the compound nucleus.

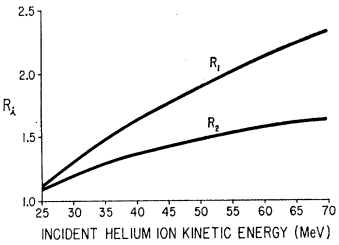

FIG. 2. Estimates of the error introduced by the assumption of Eq. (12). The curve R_1 was calculated with Eq. (18) for the emission of an α particle from the compound nucleus. The curve R_2 was calculated with Eq. (18) for the emission of an α particle resulting in a residual nucleus of one-half the excitation of the compound nucleus.

In the following discussion of the validity of the approximations we have made, we have for simplicity assumed that $T_I=1$ for $I=0$ to $I=I_{\rm max}$, and $T_I=0$ for $I>I_{\rm max}$. In the actual evaporation calculations, optical-model transmission coefficients were used.

To obtain an estimate of the error introduced by the approximation of Eq. (12) we must consider the l dependence that enters into the particle-emission probability as given by Eq. (11),

$$lT_l(\epsilon)\exp(-l^2/2\sigma^2)j_0(iIl/\sigma^2).$$

Even though the errors resulting from the approximation of Eq. (12) increase for larger values of l, the large values of l contribute relatively little to the total cross section because as l becomes large, $lT_l(\epsilon)$ approaches 0. An estimate of the error introduced into the excitation-function calculations by the approximation can be obtained from the ratio

$$R_i=\frac{\int_0^\infty lT_l{}^\nu(\epsilon)\exp(-l^2/2\sigma^2)j_0(iI_{\rm max}l/\sigma^2)dl}{\int_0^\infty lT_l{}^\nu(\epsilon)dl}. \quad (18)$$

Figure 2 shows the results of two sets of calculations of R_i. In the calculation of R_1, σ^2 was chosen to correspond to one half of the initial excitation energy, whereas in the calculation of R_2, σ^2 was chosen to correspond to the excitation energy resulting when an α particle is the first particle emitted. The particle-transmission coefficients used in both calculations were obtained with an optical-model calculation for a 10-MeV α particle. As previously stated, both results overestimate the error resulting from the assumption of Eq. (9) because $I\leq I_{\rm max}$. Figure 3 shows values of $I_{\rm av}$ for several

excitation functions calculated with

$$I_{\mathrm{av}}=\frac{\sum I(I+1)T_I(E_\alpha)P_f(E^*-\hbar^2I^2/2\vartheta_{\mathrm{rig}})}{\sum(I+1)T_I(E_\alpha)P_f(E^*-\hbar^2I^2/2\vartheta_{\mathrm{rig}})}. \quad (19)$$

As can be seen, the maximum values of I are approached only at the highest bombarding energies.

The foregoing discussion has been somewhat qualitative; unfortunately a quantitative estimate of the errors introduced by our simplifying assumptions would involve the unwieldy calculation we have tried to avoid. Our semiquantitative discussion has been based on conservative assumptions for the values of I and σ^2 and we have consequently discussed upper limits of error.

A more rigorous calculation might be based on two rather lengthy procedures. First, Bloch's use of a discrete nucleon-level nuclear model to obtain nuclear level densities would have to be applied to yield nuclear spin distributions. This extension of Bloch's nuclear level-density procedure might then be combined with a statistical theory analysis which made no simplifying assumptions about angular momentum distributions. This approach would require a prohibitively large amount of computer time.

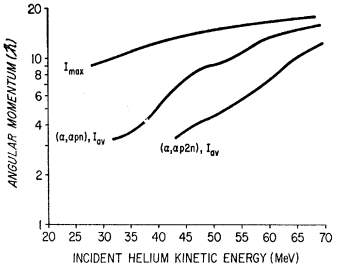

FIG. 3. Values of the maximum angular-momentum quantum number, $I_{\max}$, and average angular momentum quantum number, I_{av}, as a function of helium ion kinetic energy. The values of $I_{\max}$ were calculated classically for a point projectile that just grazes the target nucleus. The radius parameter of the target nucleus was assumed to be 1.5 F. The two curves marked I_{av}, calculated with Eq. (19), show the average value of the angular momentum quantum number for the compound nuclei of the $(\alpha,\alpha pn)$ and $(\alpha,\alpha p2n)$ reactions.

IV. RESULTS AND DISCUSSION

Experimental excitation functions for reactions of the type $(\alpha,\alpha xpyn)$ are displayed in Fig. 4. The excitation functions show the competitive behavior expected in compound nucleus excitation functions. As can be seen in Fig. 4, the Ni^{57} cross sections are small compared with Co^{57} cross sections. The $Ni^{58}(\alpha,\alpha 2n)Ni^{56}$ excitation function is not shown in Fig. 4 because the 2.6-mb maximum cross section would not be distinguishable from the abscissa.

Average recoil range measurements have been reported[14] for the reaction products Ni^{57}, Co^{57}, Ni^{56}, Co^{56}, Co^{58}, and Co^{55} which are produced by helium ion bombardment of Ni^{58}. The recoil ranges can be used to

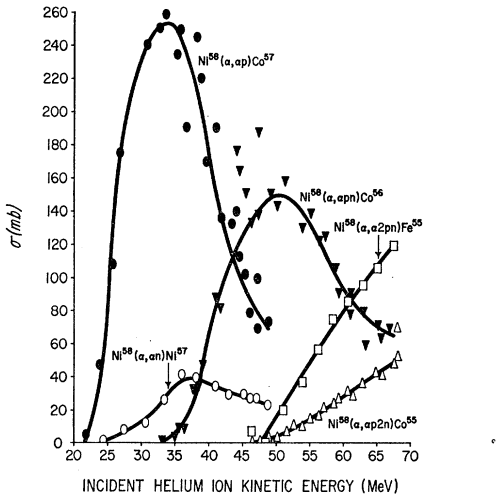

FIG. 4. Excitation functions induced in Ni^{58} with 20–68-MeV He^{++} ions. Reactions of the type $(\alpha,\alpha xpyn)$ are shown, illustrating the competitive behavior of these reactions. The $(\alpha,\alpha 2n)$ excitation function is not shown because it has a maximum cross section of 2.6 mb which would not be distinguishable from the abscissa.

determine whether or not the momentum transferred to the final residual nuclei is consistent with a compound nucleus mechanism. Where the average recoil ranges show incomplete momentum transfer, we have attempted to use the recoil ranges to set upper limits on the compound-nucleus cross sections. If we assume (1) that there is no momentum transfer in the beam direction for a direct interaction and (2) that the average measured recoil range is a linear mixture of compound-nucleus and direct interaction ranges, then the experimental cross section, multiplied by the ratio of the experimental range to the theoretical range for full momentum transfer, would equal the actual compound-nucleus cross section. This procedure only yields an upper limit for compound-nucleus cross sections because

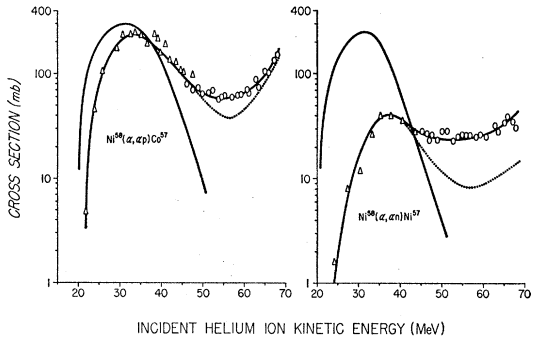

FIG. 5. Experimental and calculated excitation functions for the production of Ni^{57} and Co^{57}. Open triangles represent experimental cross sections reported in Ref. (12). Open circles represent cross sections measured in this work. Solid curves have been drawn through the experimental points for visual emphasis. The dotted curves under the excitation functions represent estimated upper limits of the compound nucleus cross sections. The estimates are based on the recoil range data of Ref. (14) as discussed in the text. The solid curves are results of standard statistical theory calculations as described in Sec. III.A of the text.

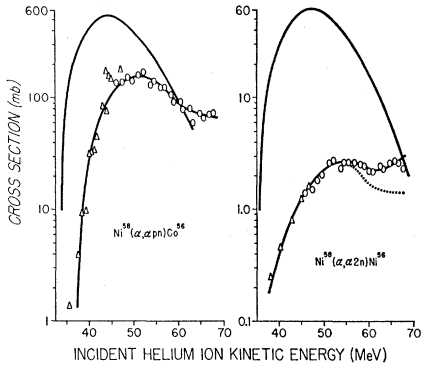

FIG. 6. Experimental and calculated excitation functions for the production of Ni^{56} and Co^{56}. Open triangles represent cross sections reported in Ref. (12). Open circles represent cross sections reported in this work. Solid curves have been drawn through the experimental points for visual emphasis. The dotted curve beneath the Ni^{56} excitation function represents an estimated upper limit of the compound nucleus cross section. The estimate is based on the recoil range data of Ref. (14) as discussed in the text. The solid curves (not passing through the experimental points) are the results of standard statistical theory calculations as discussed in Sec. III.A.

direct interactions can impart some forward range component to the recoils. The upper limits that we have calculated are indicated as dotted lines below the experimental excitation functions in the remaining figures.

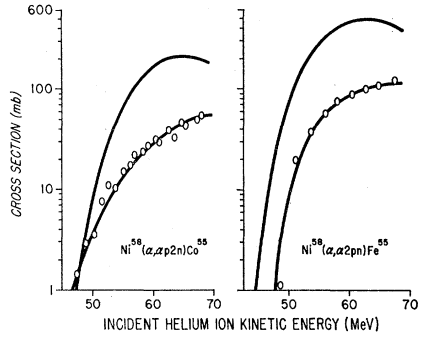

FIG. 7. Experimental and calculated excitation functions for the production of Co^{55} and Fe^{55}. Significance of curves and points is as in Fig. 6.

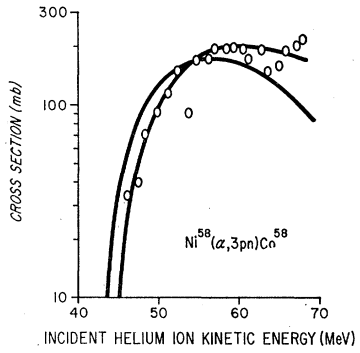

FIG. 8. Experimental and calculated excitation functions for the production of Co^{58}. Significance of curves and points is as in Fig. 6.

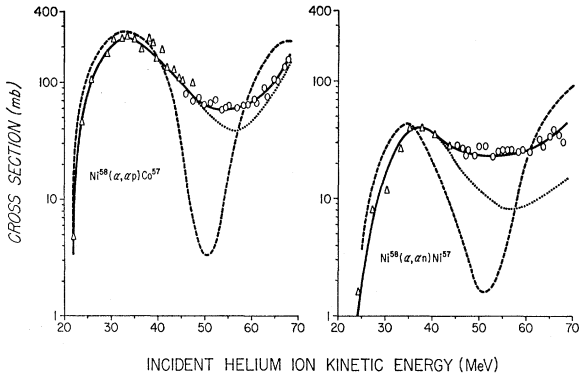

FIG. 9. Experimental and calculated excitation functions for the production of Ni^{57} and Co^{57}. Significance of experimental points is as given in Fig. 5. The dashed curves are the results of statistical theory calculations in which the influence of shell structure on level densities was considered as suggested in Ref. 18 and described in Sec. III.B.

Conventional statistical theory excitation function calculations (as described in Sec. III.A) are compared with the corresponding experimental excitation functions in Figs. 5–8. The increase (above 65 MeV) in calculated cross sections for the production of Ni^{57} and Co^{57} results from contributions of (α,5 nucleon) reactions. These calculations yield cross sections that are much greater than the experimental cross sections for the production of Ni^{56} and Ni^{57}. Similar small experimental cross sections for the production of Ni^{56} and Ni^{57} have been found in $Fe^{54}(\alpha,xpyn)$,[8] $Fe^{54}(Li^6,xpyn)$,[45] $Co^{59}(p,xpyn)$,[46] $Fe^{56}(\alpha,xpyn)$,[47] and $Ni^{58}(p,xpyn)$[48] reactions. The small cross sections for Ni^{56} and Ni^{57} production have been explained in terms of the effect of nuclear shell structure on level densities.[12,46] In addition to the difference between the magnitude of calculated and measured excitation functions, the cal-

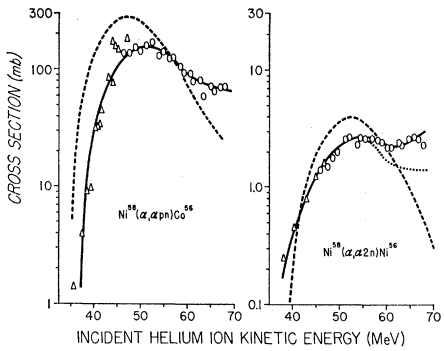

FIG. 10. Experimental and calculated excitation functions for the production of Ni^{56} and Co^{56}. Significance of curves and points is as given in Fig. 9.

[45] M. Blann, F. M. Lanzafame, and R. A. Piscitelli, Phys. Rev. **133**, B700 (1964).
[46] R. A. Sharp, R. M. Diamond, and G. Wilkinson, Phys. Rev. **101**, 1493 (1956).
[47] A. Ewart and M. Blann, Bull. Am. Phys. Soc. **9**, 471 (1964).
[48] A. Ewart, thesis, University of Rochester, 1964 (unpublished).

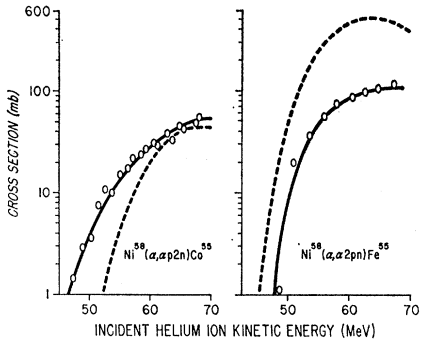

FIG. 11. Experimental and calculated excitation functions for the production Co^{55} and Fe^{55}. Significance of curves and points is as given in Fig. 9.

culated excitation functions have maxima at lower bombarding energy than the experimental curves.

Figures 9–12 show excitation functions calculated with a Rosenzweig energy shift (as described in Sec. III.B) in order to estimate the influence of shell structure on level densities. The general improvement of this set of calculations over the "standard" calculations is summarized in Table III.

TABLE III. Ratios of maximum calculated yields to maximum experimental yields.

Reaction	Standard calculation	Rosenzweig calculation
$Ni^{58}(\alpha,\alpha n)Ni^{57}$	6.1	1.1
$Ni^{58}(\alpha,\alpha p)Co^{57}$	1.1	1.1
$Ni^{58}(\alpha,\alpha 2n)Ni^{56}$	23.0	1.5
$Ni^{58}(\alpha,\alpha pn)Co^{56}$	3.4	1.7
$Ni^{58}(\alpha,\alpha p2n)Co^{55}$	3.8	0.80
$Ni^{58}(\alpha,\alpha 2pn)Fe^{55}$	4.5	4.9
$Ni^{58}(\alpha,3pn)Co^{58}$	0.86	1.2

Excitation functions calculated with Eq. (10) are presented in Figs. 13 and 14 for the $(\alpha,\alpha p)$, $(\alpha,\alpha pn)$, and $(\alpha,\alpha p2n)$ reactions; we have attempted to consider the influence of angular momentum on nuclear level

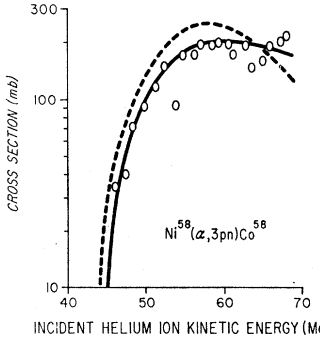

FIG. 12. Experimental and calculated excitation functions for the production of Co^{58}. Significance of curves and points is as given in Fig. 9.

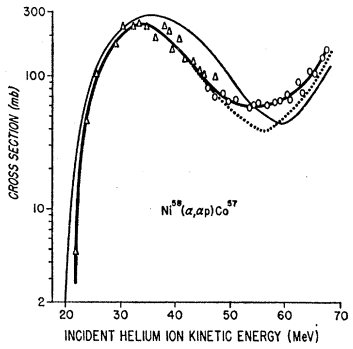

FIG. 13. Experimental and calculated excitation functions for the production of Co^{57}. Significance of experimental points is as given in Fig. 5. The thin solid curve is the result of a calculation in which the influence of angular momentum on level densities was considered, as discussed in Sec. III.C.

densities in these calculations as described in Sec. III.C. Similar calculations for the other reactions measured have not been presented, since the changes with respect to the standard calculation are analogous to the changes in the reactions presented in Figs. 13 and 14. Comparison of Figs. 13 and 14 with Figs. 5–7 shows that the result of the third set of calculations is to shift the calculated excitation functions to higher energy, and to broaden them as well. Both effects are in the direction of improved agreement with the experimental excitation functions, although it appears there may actually be a degree of overcorrection in the third set of calculations. This is not unreasonable when the extreme nature of the assumptions going into these calculations is considered.

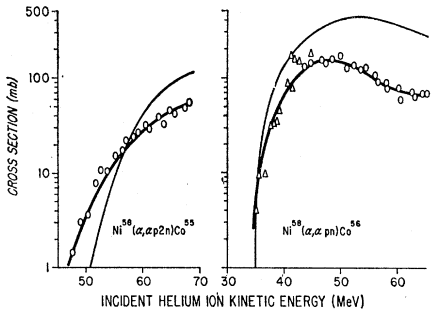

FIG. 14. Experimental and calculated excitation functions for the production of Co^{56} and Co^{55}. Significance of experimental points is as given for Fig. 5; significance of thin solid curves is as given in Fig. 13.

V. CONCLUSIONS

The experimental excitation functions of this work have been compared with three sets of statistical theory calculations. The parameters used in the calculations were taken, where possible, from independent experimental determinations.

The first set of calculations was performed with the commonly used formulation of the statistical theory as described by Weisskopf.[15] The excitation functions so

calculated were somewhat narrower, and peaked at lower energies than the experimental excitation functions. Even more striking was the error in the magnitude of the calculated excitation functions for nuclides near the doubly magic Ni^{56} nucleus. This error has been noted for a large number of target-projectile systems yielding the same product nuclides measured in this work; a consistent explanation is that the level densities of these nuclides are influenced by shell structure, even at reasonably high excitation energies.

The second set of calculations employed a level-density expression in which the influence of shell structure on level densities was taken into consideration in the manner suggested by Rosenzweig. The agreement between calculated and experimental peak cross sections was generally improved in the second set of calculations, as is summarized in Table III.

In the third set of calculations two simplifying assumptions were made in considering the influence of large values of angular momentum on the decay of highly excited nuclei. The excitation functions calculated in this fashion were broadened, and shifted to higher excitation energies compared with those of the first set of calculations.

On the basis of the comparisons of the calculated and experimental excitation functions of this work, we find no reason to abandon the concept of the statistical model up to the highest energies encountered in this work.

VI. ACKNOWLEDGMENTS

We are grateful to H. Grunder and the crew of the Lawrence Radiation Laboratory 88-in. cyclotron for the bombardments in this work, and to the Chemistry Division of LRL for permitting us to use the facility while one of the authors (M.B.) was a visitor at the laboratory. We appreciate the kind help and hospitality of Dr. Max Goldstein and Dr. Henry Mullish of the New York University Computing Center for aid in performing the machine calculations of this work. Helpful discussions with Professor J. B. French and Professor T. D. Thomas were also very much appreciated. We wish to thank L. Schwartz and J. Cooper for the drawings of this work. The authors gratefully acknowledge a critical reading of the manuscript by Professor L. Winsberg and Professor J. Huizenga.

PHYSICAL REVIEW VOLUME 137, NUMBER 2B 25 JANUARY 1965

Effect of β Vibrations on Multiple Coulomb Excitation Within the Ground-State Band*

H. G. WAHSWEILER†
Yale University, New Haven, Connecticut
(Received 1 September 1964)

Alder and Winther's theory of multiple Coulomb excitation is applied to the rotation-vibration model of axially deformed nuclei. It is shown that in the transition region of deformed nuclei one can account in this way for the differences between values obtained from experiments and the theoretical excitation probabilities of the rotational model.

I. INTRODUCTION

MANY levels of the nuclei in the region $150<A<190$ can be classified as rotational bands built on collective vibrations with the two shape parameters β and γ.[1] A considerable amount of experimental information on these bands was obtained[2] in Sm^{152}. Theoretical investigations which confirm the view that the deformed nuclei have predominantly a prolate-spheroidal equilibrium shape were carried out by Yamazaki[3] and by Gupta and Preston.[4] The so-called "rotation-vibration-interaction" for axially symmetric nuclei was investigated in detail by Faessler and Greiner[5–7] and by Preston and Kiang[8]; according to these views this interaction can cause mixing different rotational bands. Nielson[9] as well as Greenberg *et al.*[10] found that the gamma-band admixture to the ground-

* Supported by the U. S. Atomic Energy Commission under Contract AT (30-1)-1807.
† Now at the Institute for Theoretical Physics, University of Tübingen, Tübingen, Germany.
[1] R. K. Sheline, Rev. Mod. Phys. **32**, 1 (1960).
[2] J. S. Greenberg, D. A. Bromley, G. C. Seaman, and E. V. Bishop, *Proceedings of the Third Conference on Reactions Between Complex Nuclei, Asilomar, California*, edited by A. Ghiorso, R. M. Diamond, and H. E. Conzett (University of California Press, Berkeley, California, 1963), p. 295.
[3] T. Yamazaki, Nucl. Phys. **49**, 1 (1963).
[4] S. Das Gupta and M. A. Preston, Nucl. Phys. **49**, 401 (1963).
[5] A. Faessler and W. Greiner, Z. Physik **168**, 425 (1962).
[6] A. Faessler and W. Greiner, Z. Physik **170**, 105 (1962).
[7] A. Faessler and W. Greiner, Z. Physik **177**, 190 (1964).
[8] M. A. Preston and D. Kiang, Can. J. Phys. **41**, 742 (1963).
[9] O. B. Nielson, *Proceedings of the Rutherford Jubilee International Conference* (Heywood and Company, Ltd., London, 1961), p. 317.
[10] J. S. Greenberg, G. C. Seaman, E. V. Bishop, and D. A. Bromley, Phys. Rev. Letters **11**, 211 (1963).